AUSTRIAN JOURNAL of EARTH SCIENCES
[MITTEILUNGEN DER ÖSTERREICHISCHEN GEOLOGISCHEN GESELLSCHAFT]

AN INTERNATIONAL JOURNAL OF THE AUSTRIAN GEOLOGICAL SOCIETY
VOLUME 97 2004   2005

3-D seismic interpretation and structural modeling in the Vienna Basin: implications for Miocene to recent kinematics.

R. HINSCH[1)*)], K. DECKER[1)] & H. PERESSON[2)]

[1)] Department of Geological Sciences, University of Vienna, Althanstrasse 14, 1090 Vienna, Austria
[2)] OMV AG Austria, Gerasdorfer Strasse, 1210 Vienna, Austria
[*)] Corresponding author, present address: Rohoel-Aufsuchungs AG (RAG)
   Schwarzenbergplatz 16, 1015 Vienna, Austria, ralph.hinsch@rohoel.at

Abstract

The current paper focuses on the construction of an integrated 3-D model comprising the most important fault systems of the Vienna pull-apart basin. The model is constructed from geological interpretations of 3-D seismic data, digitized structural maps of the pre-Tertiary basin floor, Quaternary thickness maps, earthquake and digital elevation data. The spatial model is used for the assessment of the Miocene and Quaternary fault kinematics. The results indicate several important differences between Miocene and active tectonics, although both deformations occurred under grossly similar boundary conditions.

Miocene deformation is characterized by the formation of a thin-skinned pull-apart basin, which subsides at a major left overstep of the sinistral Vienna Basin transfer fault extending from the Eastern Alps (Mur-Mürz Fault) into the Outer Carpathians. Large-scale fault modeling of this basin indicates that the position of both oversteps and the pull-apart is spatially linked to the morphology of the overthrust autochthonous European basement below the thin-skinned fault system. The thickest growth strata inside the pull-apart accumulate adjacent to the Steinberg normal fault system, which forms the major kinematical linkage between the overstepping strike-slip faults. Main subsidence during the Lower Sarmatian and the Lower Pannonian occurs in the centre of the pull-apart between the Steinberg and Bockfliess Faults.

During Quaternary deformation many of the Miocene faults are reactivated. Quaternary sedimentary basins, tectonic geomorphology and seismicity patterns highlight the recent sinistral transfer fault, which is located at the eastern border of the Miocene pull-apart. This active strike-slip fault shows up as an almost linear feature without major oversteps continuing from the Mur-Mürz Fault into the Little Carpathians. Small-scale releasing bends along this fault are aligned with negative flower structures, which contain thick Quaternary basins (Mitterndorf- and Lassee Basin). Active normal faulting with slip rates far below the Miocene ones occurs at faults in the hanging-wall of the Steinberg Fault in the central Vienna Basin and likely on the Steinberg Fault itself. These faults seem to be kinematically linked to the active strike-slip fault via a common detachment plane. The normal faults, however, do not link between major overstepping fault segments as previously in the Miocene but can be understood as part of a large scale asymmetric flower structure.

Die Arbeit enthält ein integriertes 3-D Modell der wichtigsten Störungssysteme des Wiener Beckens, das aus geologischen Interpretationen von 3-D Seismik, digitalisierten Strukturkarten des Beckenuntergrundes, Quartärmächtigkeitskarten, Erdbebendaten, sowie einem digitalen Geländemodell abgeleitet wird. Das räumliche Modell bildet die Grundlage für die Bewertung der Kinematik der abgebildeten Störungssysteme. Die Interpretation der in ihrem räumlichen Zusammenhang visualisierten Daten deutet darauf hin, dass sich miozäne und quartäre Kinematik im Wiener Becken zwar ähnlich sind, sich in einigen wichtigen Punkten aber unterscheiden.

Die miozäne Kinematik ist durch die Bildung eines thin-skinned *pull-apart* Beckens an einer linksseitig übertretenden sinistralen Transferstörung zwischen Ostalpen (Mur-Mürz-Störung) und Karpaten gekennzeichnet. Die großräumige Störungsmodellierung im Bereich des Wiener Becken zeigt, daß die Position dieses Beckens zwischen Alpen und Karpaten durch die Untergrundstruktur des überschobenen europäischen Plattenrandes bestimmt wird. Zwischen Unterem Sarmat und Unterem Pannon akkumulieren die mächtigsten syntektonischen Sedimente in der Hangendscholle des Steinberg-Bruchsystems, der die kinematische Verbindung zwischen den übertretenden Seitenverschiebungen herstellt. Die mächtigsten Sedimente liegen zwischen dem Steinberg-Bruch und dem Bockfließer Störungssystem im Zentrum des *pull-apart* Beckens.

Im Quartär sind viele der miozänen Störungen weiterhin aktiv. Die aktive sinistrale Transferstörung ist jedoch an den Ostrand des Wiener Beckens verlagert, wie sich aus störungsgebundenen quartären Sedimentbecken, Geomorphologie und Seismizität ableiten lässt. Das quartäre und rezente Transfersystem setzt sich geradlinig und ohne *pull-apart* Übertritt in einer NE-streichenden Störungszone in die Kleinen Karpaten fort. Kleinere Releasing Bends an der Transferstörung sind durch Abschiebungen in negativen Blumenstrukturen (negative flower structures) und mächtige quartäre Becken (Mitterndorfer Becken, Lasseer Senke) markiert. Die fortgesetzte, gegenüber dem Miozän jedoch wesentlich langsamere Bewegung von Abschiebungen im zentralen Wiener Becken deutet auf die anhaltende kinematische Koppelung des Steinberg-Bruches mit der seismisch aktiven Transferstörung über einen gemeinsamen Abscherhorizont hin.

1. Introduction

The understanding of processes, which are linked to crustal deformation more and more relies on various balancing techniques as well as on physical modeling. Such structural and physical quantifications need as many quantitative constraints for the setup of appropriate models as possible. One major group of important input data is the spatial geometry of geological

surface and subsurface structures. Well-defined three-dimensional geometries of faults and stratigraphic horizons in many cases put constraints on kinematical interpretations of the processes, which are tight enough to discriminate between alternative interpretations of formational mechanisms of certain tectonic structures. Such well-elaborated spatial data therefore already by themselves contain important kinematical and partly even mechanical information on the processes active. The integration of various datasets in a coherent 3-D data model is not only regarded as a simple visualization tool but rather as a firm basis for interpreting structural processes. Spatial visualization is capable to shed light on the relation between structures, which is sometimes not clearly detectable in map or cross sections. Furthermore visualization serve as a tool to detect relations between different data sets, which otherwise are hidden or unclear.

The purpose of this paper is to present an elaborated example of spatial data integration from the surface and subsurface of the Vienna Basin and the adjacent areas in Eastern Austria. Major parts of the presented digital three-dimensional data base have been created in the last three years using various sources of geological and geophysical subsurface data including structural maps (Kröll and Wessely, 1993; Wessely et al., 1993; Kröll et al., 2001), 3-D seismic and well data by OMV, and earthquake data (ZAMG, 2001, 2004). Data integration was performed to backup interpretations on the active tectonics of the Vienna Basin Transfer Fault. The results of these studies have been published elsewhere (Hinsch and Decker, 2003; Decker et al., 2005; Hinsch et al., 2005). In the present paper we focus on the methodology of spatial data modeling and on the workflow leading to coherent 3-D data models containing data of different types, origins and reliabilities. Data examples and resulting interpretations are discussed in the frame of existing models of the Vienna Basin system focusing on some important differences between the Miocene and recent kinematics of the transfer system.

1.1. Regional background

The Miocene Vienna pull-apart basin evolved between two left-stepping segments of a major sinistral transform system with basin subsidence starting during the Early Miocene (Sauer et al., 1992). The structural styles within the pull-apart are dominated by extensional strike-slip duplexes and by en-echelon normal faults connected to strike-slip faults. Strike-slip faults are characterized by NNE-oriented extensional duplexes with overstepping NE-striking sinistral faults, which are connected by N(NE)-striking oblique sinistral faults. Such geometries are characteristic for both surface faults and fault polygons depicted in subcrop maps and seismic data (Decker, 1996). The main structures causing the rapid subsidence of the Miocene pull-apart basin are faults located close to the W and NW boundary of the basin such as the Leopoldsdorf and the Steinberg Faults with up to 4.2 and 5.6 km normal offset, respectively. These faults are kinematically linked to the strike-slip systems and associated with growth strata, which date the normal fault activity as Karpatian to Pannonian (c. 17 - 8 Ma; Sauer et al., 1992; Fodor, 1995; Lankreijer et al., 1995). The faults are thought to root in the Alpine-Carpathian floor thrust (Royden, 1985; 1988; Wessely, 1988; 1993). The Miocene offset along the fault system in the Mur-Mürz-Vienna Basin area has been estimated with 30 - 40 km (Fig. 2; Linzer et al., 2002).

The following chapters describe detailed spatial structural models from the southern and central Vienna Basin with data covering two distinct structural settings in the basin. These are the major strike-slip system in the southern Vienna Basin and the normal fault system close to the western boundary of the central Vienna Basin.
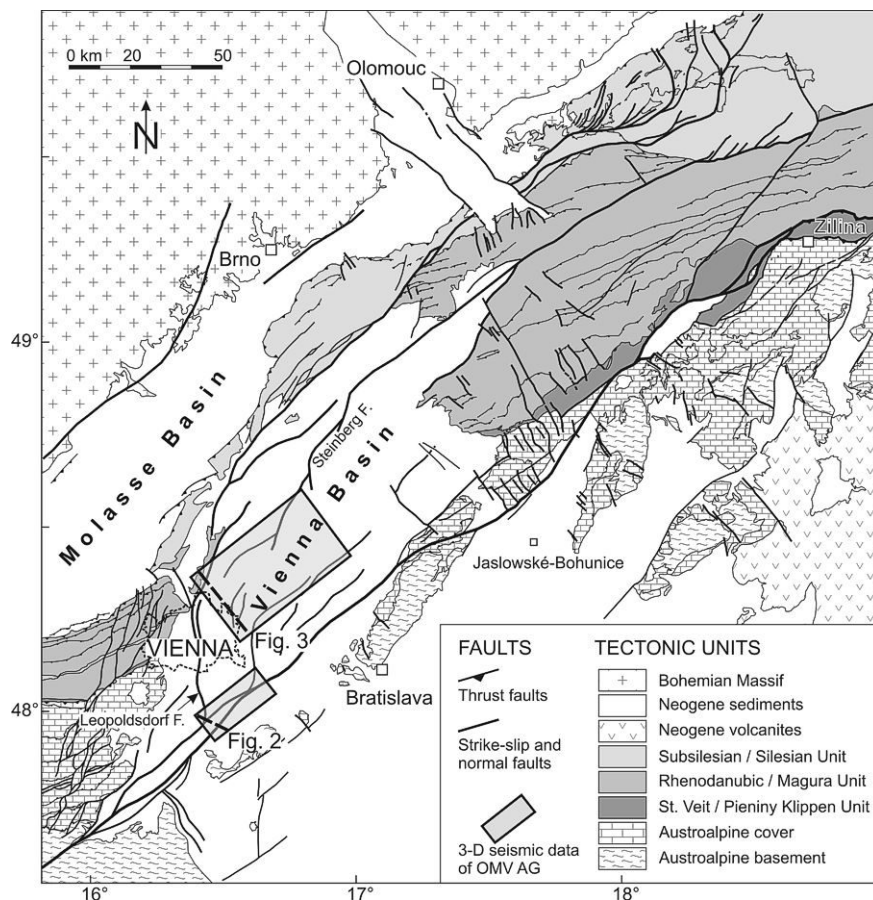

Figure 1: Tectonic map of the Vienna Basin and its surrounding. Synthesized from Geological Maps of Austria (1:50.000), former Czechoslovakia (1:200.000), Fuchs and Grill (1984) and Kröll and Wessely (1993). The position of the 3-D seismic data volumes from OMV Austria AG, on which work has been done, is indicated (southern block = 3D Moosbrunn, northern block = 3D SAYMATZDUE).

2. Assessing the spatial fault and horizon geometry in the Vienna Basin

In this paragraph the database, the interpretation and the structural modelling leading to a subsurface spatial model of the Vienna Basin and surroundings are described. Main inputs come from 3-D seismic interpretations of data, which have been provided by OMV AG, Austria. Additional published data is integrated to provide a framework for visualization and regional kinematical interpretation. Data is integrated in the discrete modeling software GOCAD after being constructed or elaborated by other applications. These processing steps are discussed in the following chapters.

2.1. Fault and horizon mapping in the southern Vienna Basin (3-D seismic block Moosbrunn)

The time migrated 3-D reflection seismic block Moosbrunn images the Miocene basin fill of the southern Vienna Basin with a coverage of c. 190 km² and a recording time of 3 s TWT (Fig. 2). Stratigraphic ties of imaged horizons are provided by 3 wells (Fig. 2; all data by OMV AG, Austria). The 3-D block has been thoroughly mapped with respect to fault geometries and stratigraphic horizons. The main objective of that work was to map the seismotectonically active faults by integrating the seismic interpretation with near surface data on the tectonic
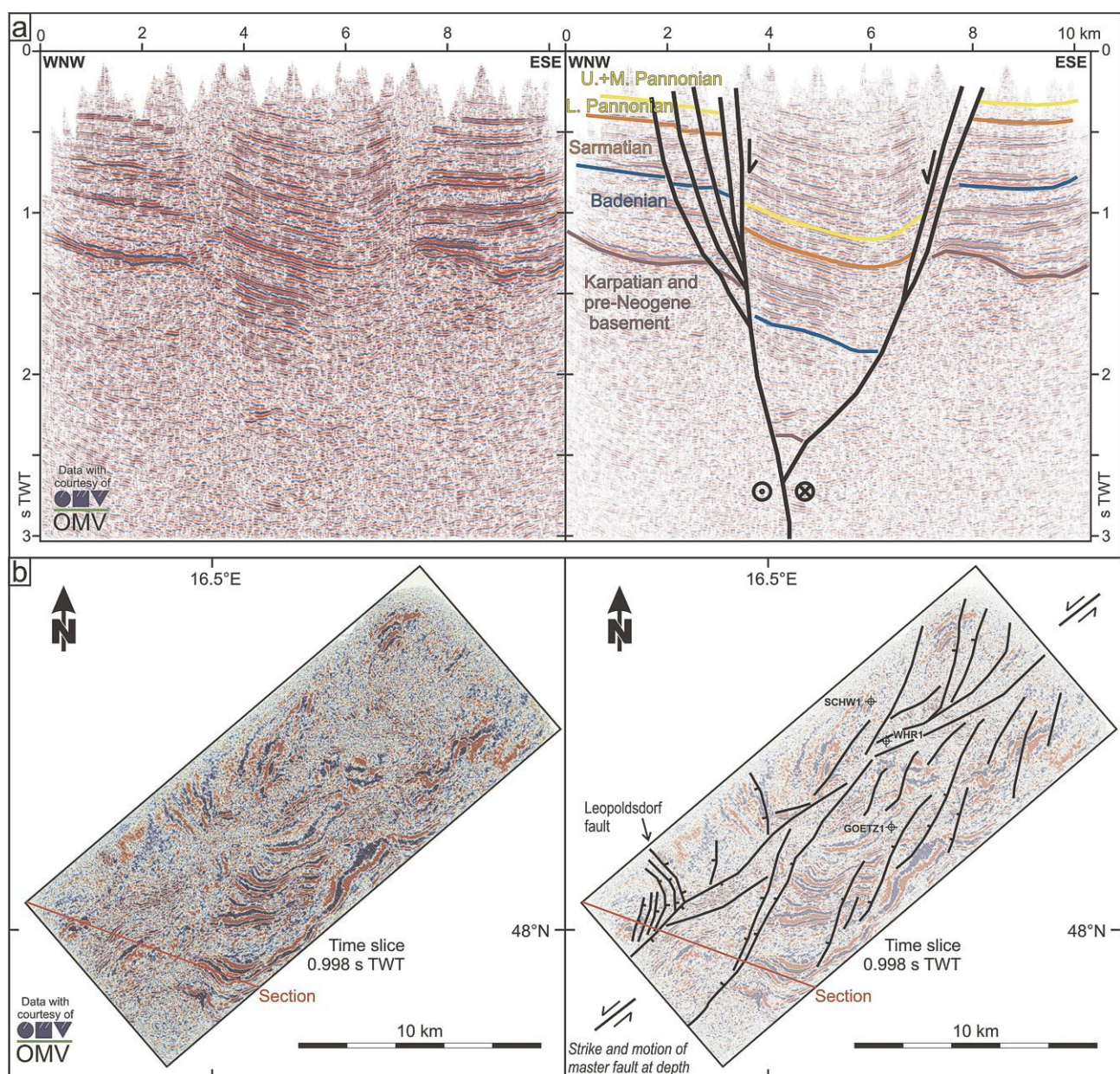

Figure 2: 3-D seismic interpretation in the southern Vienna Basin (3D Moosbrunn of OMV Austria AG), for location see Figure 1.
a) Seismic section (left) and interpretation (right) revealing a negative flower structure. Vertical exaggeration is approx. 2.5 at 2 s TWT (modified from Hinsch et al., 2005).
 b) Time slice (left) and interpretation revealing a complex fault system of strike slip and normal faults attributed to sinistral transtensional movements on a master fault at depth.

geomorphology and Quaternary sediments, which accumulated in fault-bounded basins. The main results are published by Decker et al. (2005) and Hinsch et al. (2005). Additional detailed stratigraphic interpretations of the eastern part of the 3-D block revealed a refined sequence stratigraphy framework for the Miocene of the southern Vienna Basin (Strauss et al., 2004, 2005). The stratigraphic architecture derived from these analyses provide good time constraints for the complex history of faulting in that part of the Vienna Basin.

Figure 2 shows examples of the 3-D seismic data Moosbrunn and its interpretation. Cross-lines reveal a negative flower structure with boundary faults, which converge to depth (Fig. 2a). The central part of the structure is vertically displaced for up to 1 s TWT with respect to the boundaries of the fault zone. Throughout the cube Neogene sediments are imaged by continuous reflectors, while the pre-Neogene basement is somewhat noisy without major reflections. According to Wessely et al. (1993) the basement is formed by Austroalpine thrust sheets (Calcareous Alps: west of the 3-D survey; Paleozoic Grauwacken Unit: central part of the basin; Austroalpine crystalline units: eastern part).

Fault traces of the depicted flower structure have been systematically mapped in cross-lines at a spacing of 125 m. In complex areas more cross-lines with closer spacing were used. The correlation of fault traces considered faults mapped in cross-lines, time slices and seismic attribute maps. Map-views of the fault system display a major fault zone in the central part of the block and several branch faults (Fig. 2b). Intense fracturing along the major faults is indicated by low reflectivity and offset non-continuous reflections. Several minor faults branch off from the main fault zone in an en-echelon-pattern. The poor reflectivity imaged in a large part of the northern portion of the time slice, however, is due to seismic acquisition rather than to structural or stratigraphic changes. The lower quality results in fault traces, which are somewhat more ambiguous than those mapped in the southern part of the block.

In order to quantify vertical fault displacements and to visualize fault offsets a stratigraphic horizon has been mapped in the seismic data (Fig. 2a). The horizon chosen is the top of the Upper Sarmatian

(c. 11.5 M yrs), which can be mapped in all fault-bounded blocks of the seismic data by seismic pattern and sequence analysis with adequate accuracy.

2.2. Fault and horizon mapping in the central Vienna Basin (3-D seismic block Seyring-Matzen-Dürnkrut)

The 3-D block SAYMATZDUE of OMV AG is a merged time migrated 3-D reflection seismic dataset covering large parts of the central Vienna Basin with an extent of about 840 km². The fault and horizon model presented here is mainly based on an interpretation campaign, which was conducted on in-house systems of OMV (Hinsch, 2003). In order to get information on the Miocene to younger deformation history that is imaged in the seismic data a lower Sarmatian and a lower Pannonian horizon, which is relatively close to the surface (0 - 750 ms TWT), is mapped. Figure 3 shows an example of the seismic interpretation.
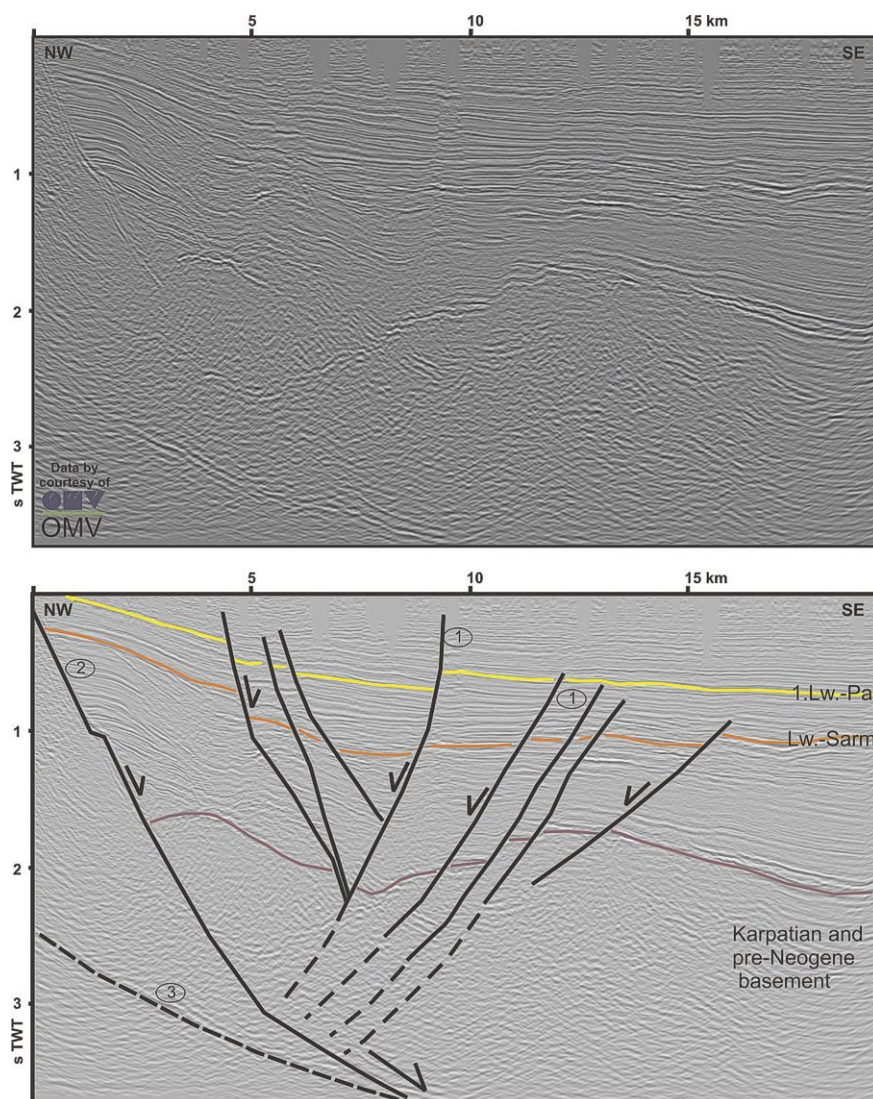

Figure 3: 3-D seismic interpretation in the central Vienna Basin. Seismic section (top) and interpretation (lower) revealing a part of the extensional fault of the Miocene pull-apart evolution. 1.Lw.-Pa. = Top First Lower Pannonian; Lw.-Sarm = Top Lower Sarmatian; Vertical exaggeration is approx. 2.4 at 2 s TWT. 1: Aderklaa-Bockfliess Fault System; 2: Bisamberg Fault; 3: Alpine floor thrust.

Horizon mapping is amended by an ample fault trace interpretation (Fig. 3b), which is used to obtain a generalized fault model.

Cross-sections display a major east-dipping normal fault (Bisamberg Fault) with syn- and antithetic normal faults deforming the hanging wall (Aderklaa-Bockfliess Fault System, Fig. 3). The fault system offsets the pre-Neogene basement for about 2.2 s TWT (c. 3000 m; Fig. 3, km 8). Faults rooting in the former main thrust of the alpine wedge, which is probably imaged in the lower left part of the section. The five antithetic faults depicted show distinct timing of fault activities during the Miocene with faults becoming systematically younger towards NW (Fig. 3b). Offset marker horizons show that slip at the south-eastern fault terminated between the Upper Sarmatian and the Lower Pannonian, which is not offset by the fault. The three antithetic

faults further NW offset the Lower Pannonian, but terminate in the overlying sequence, and the north-western fault is traced upwards to the top of the seismically imaged layers (i.e., to c. 200 ms TWT).

2.3. Modeling of mapped faults and horizons

All fault traces interpreted from seismic data are imported into GOCAD (Fig. 4b). The fault surfaces are created according to the description in Appendix 3, accordingly not all fault traces have been regarded and the fault surface model is a generalized one (Fig. 4c). In order to visualize fault offsets stratigraphic horizons, which have been mapped in the seismic data are also used to create modeled surfaces in GOCAD (Fig. 4d).

2.3.1. Calculation of Lower Sarmatian to Lower Pannonian vertical thickness

The two mapped horizons in the Central Vienna Basin (Top Lower Sarmatian and Top First Lower Pannonian Horizon, Fig. 5 a, b) are used to calculate their vertical distance. This vertical thickness is a first approximation of the sediment thickness between these horizons. Normal faults, which were active between the Lower Sarmatian and the Lower Pannonian are highlighted by thick growth strata along faults. Thickness values cannot be calculated for the areas between the hangingwall cut-off of the lower horizon and the footwall cut-off of the upper horizon (Figs. 5c, 6). For these areas values are interpolated and the resulting vertical thickness calculation is only an approximation of the true stratigraphic thickness. The final map of vertical thickness is displayed in Figure 5d. Normal faults, which were active between the Lower Sarmatian and the Lower Pannonian (i.e., during an estimated time span of 2 - 3 Ma; compare Rögl, 1996), are highlighted by thick growth strata along faults.

The map of vertical thickness between the top First Lower Pannonian horizon and top Lower Sarmatian (Fig. 5) displays a depocenter of growth strata on the hanging wall of the west-dipping Bockfliess Fault with up to 1100 m sediments. Additional thick accumulations of sediments are indicated north of the Matzen Faults on the
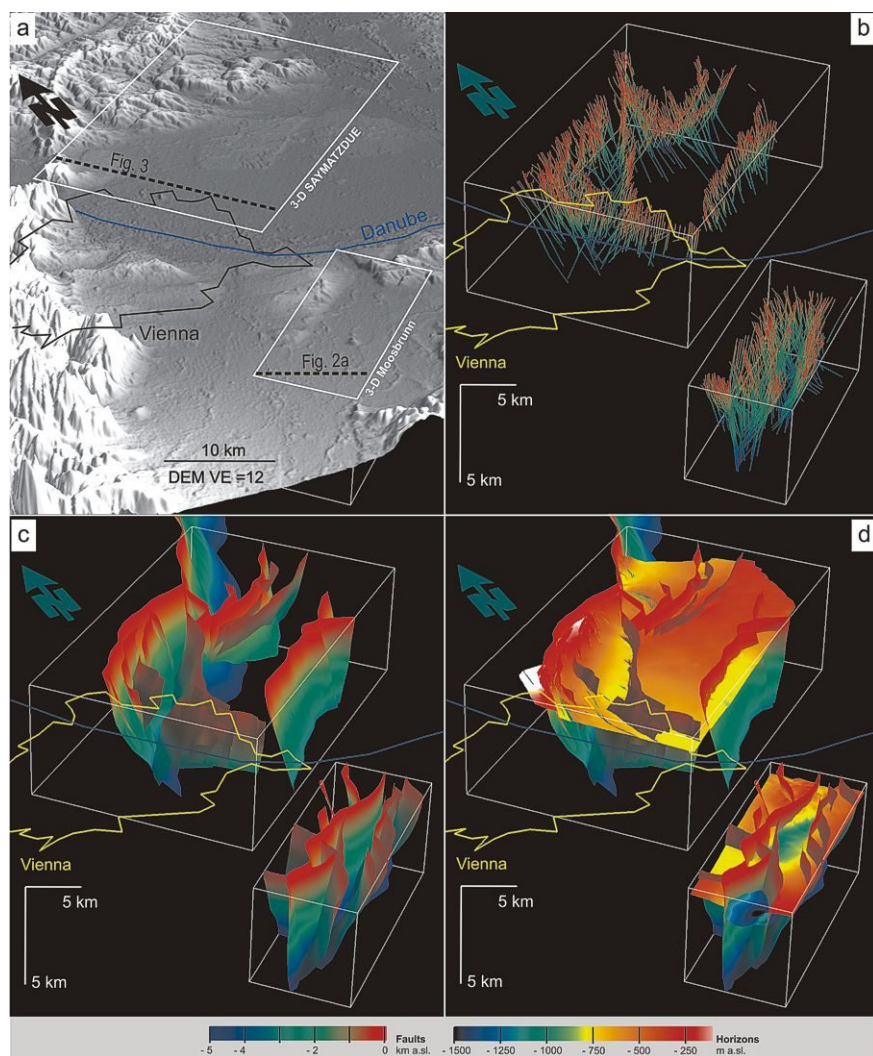

Figure 4: Modeling of faults and horizons from 3-D seismic interpretation data.
a) Oblique view of an exaggerated digital elevation model of the area displayed in b-c. The city limits of Vienna are given for orientation purposes. Vertical exaggeration = 12.
b) Oblique view of the fault traces interpreted in reflection seismic surveys in the southern and central Vienna Basin used for construction of fault surfaces.
c) Fault surfaces created from fault trace information, partly generalized.
d) Combined display of faulted horizons and fault surfaces, giving an instant visualization of fault kinematics. In the northern data block the original picked horizon (Lower Pannonian) is displayed, showing that the modeled fault surfaces represent a generalization. In the southern data block the displayed horizon (Upper Sarmartian) is refitted to the modeled faults.

northernmost limit of the map in the hanging wall of the east-dipping Steinberg Fault. The Bockfliess and Steinberg Faults are thus the most active faults in the time span represented by the vertical thickness.

Growth strata thickness is used to approximate slip rates of the normal faults during the Late Miocene (i.e the Lower Sarmatian to Lower Pannonian). A gross estimate of normal slip rates reveals a maximum 0.37 - 0.55 mm vertical slip per year for the Bockfliess Fault (max. growth strata thickness 1100 accumulated during 2 - 3 Ma) and 0.20 - 0.30 mm for the Markgrafneusiedl Fault (max. 600 m growth strata). We are aware that the calculation of slip rates from stratigraphic thickness does not account for sediment compaction and calculated values are to low. Further uncertainties come from the quality of time to depth conversion. However, calculated values are in the same order than vertical slip rates calculated from well data for the Bisamberg, Aderklaa and Markgrafneusiedl faults (Wagreich and Schmid, 2002), ranging from 0,1-0,4 mm/yr. These velocities are slightly lower than values calculated from the seismic horizons, because their transect of wells does not cross the depocenter.

Another interesting fact to note is, that the Bockfliess Fault is west-dipping while its linear prolongation to the north, the Steinberg Fault is east dipping.

2.4. Integration and compilation of existing data

Published surface and subsurface data is integrated into the 3-D structural database obtained from seismic interpretation and structural modeling. This is done to allow combined spatial visualization of the different data sets to back-up kinematical interpretations of the faults active in the upper crust.

Data derived from published and unpublished subsurface maps (Tab. 1). The data has been digitized and geo-referenced to allow import into GOCAD. Contour lines are used to create GOCAD surfaces by DSI interpolation (see Appendix).

2.5. Large scale structure of the Vienna Basin area

In order to assess and visualize

the large scale structure of the Vienna Basin fault system additional fault surfaces have been constructed.

Three major normal faults, the Leopoldsdorf Fault, an eastern branch fault of the Leopoldsdorf Fault, and the Steinberg Fault have been constructed in areas outside the available 3-D seismic data (Fig. 7b). These faults are constructed from the fault heaves of the surface representing the base of Neogene basin fill, which cover the entire Vienna Basin (Kröll and Wessely, 1993, Fig. 8b, Tab. 1). These faults are linked to the fault segments mapped in the 3-D seismic data. These basin-wide fault data is amended with a surface representing the top of the autochthonous pre-Miocene sediments on the Bohemian Massif below the Alpine thrust sheets and the Vienna Basin as described in the following.
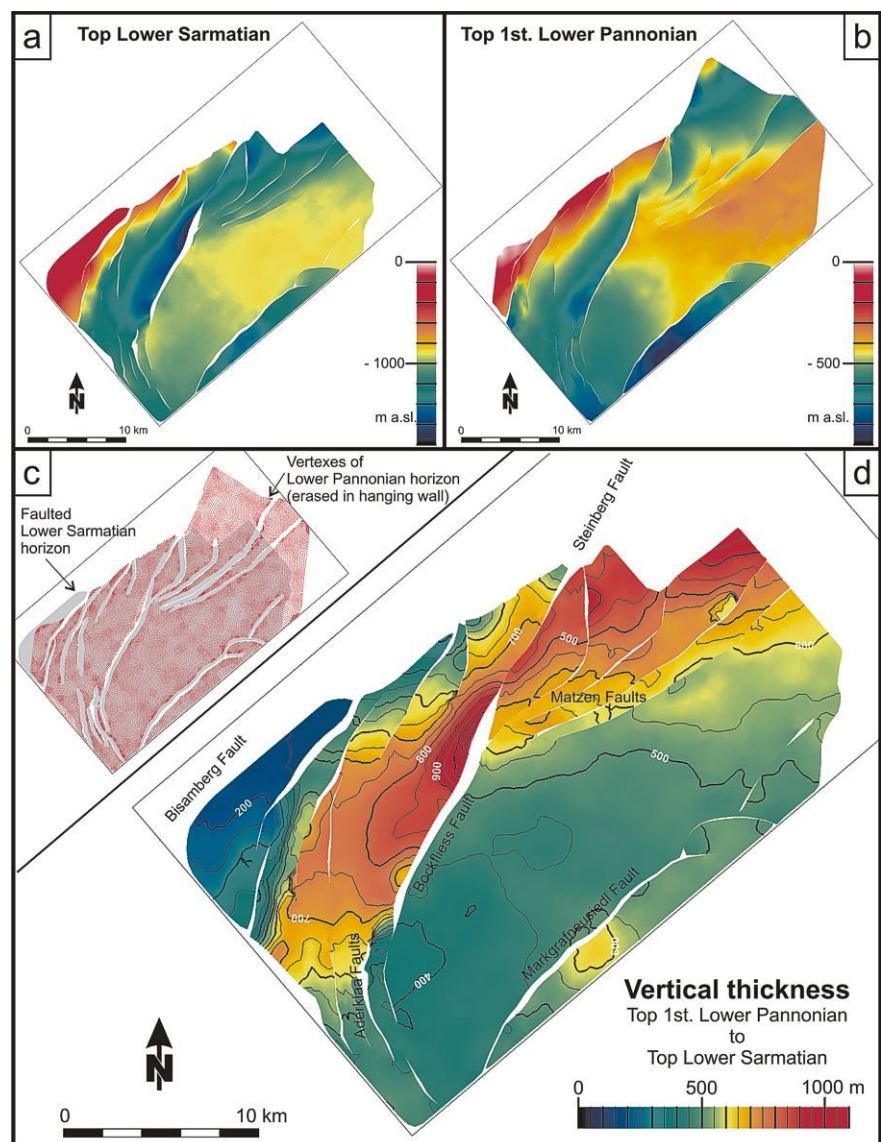

FIGURE 5: Calculation of vertical thickness between two Miocene horizons.
a) Depth structure of the Top Lower Sarmatian horizon. The horizon has been fitted to the modeled faults.
b) Depth structure of the Top First Lower Pannonian. This horizon has also been fitted to the modeled faults.
c) Vertexes of the First Lower Pannonian horizon (red) superposed on the map-shape of the Top Lower Sarmatian Horizon. Vertexes of the hanging wall close to the faults have been deleted to avoid miscalculated thickness values (c.f. Fig. 6).
d) Contour map of calculated vertical thickness between Top Lower Sarmatian and Top First Lower Pannonian. Areas of null values close to faults have been interpolated.

Data	Data type / description	Source	
SRTM derived Digital Elevation Model	Digital Elevation data with 90 m horizontal resolution	USGS-NIMA (2003)	Fig. 7a
Base of Quaternary gravels / Mitterndorf Basin	Contour map, scale 1:25.000	Berger (1987)	Fig. 7b
Base of Quaternary gravels / Marchfeld area	Contour map, scale 1:50.000	DOKW (1984)	Fig. 7b
Base of Quaternary gravels / Zohor Basin	Series of cross-sections, scale 1:100.000	Kullmann (2000)	Fig. 7b
Base of the Neogene basin fill of the Vienna Basin	Contour map with fault heaves, scale 1:200000	Kröll and Wessely (1993)	Fig. 8b
Base of the molasse in Lower Austria and adjacent areas	Contour map with fault heaves, scale 1:200000.	Kröll et al. (2001)	Fig. 8b

TABLE 1: Table 1 Overview of major data imported into GOCAD.

2.5.1. Generalized top of the European Plate

The molasse sediments of the foreland basin in front of the Alpine thrust system overly the autochthonous Mesozoic sediments and the crystalline basement of the European lower plate. Both the foreland basin and the European plate dip south below the Alpine thrust sheets and the Vienna Basin (compare cross sections by Wessely, 1987 and Kröll et al., 2001). Thus, the base of molasses sediments mimic the shape of the top of the European plate. Furthermore, the molasse is relatively thin underneath the alpine wedge, hence the surface representing the molasses basin base also approximates the trend the basal detachment of the Alpine thrust system (Table 1, Fig. 8b).

In order to model this plane, the surface representing the base of the molasse sediments (Kröll et al., 2001) is smoothed and generalized by utilizing GOCADs DSI smoothing to fit a very rough triangulated surface through the original contoured surface (Fig. 9a). In a second working step, this generalized trend is extrapolated and the surface extended. The resulting surface now represents the trend of the European plate underneath the Vienna Basin (Fig. 10).

Because flexural bending of the lower plate is not regarded in the extrapolated part of the surface, the generalized surface is just a first order approximation of the top of the European platform. Thus, with increasing distance of extrapolation the modeled surface becomes more speculative and probably is situated in a position too high and with too shallow dip. Deep seismic profiles, refraction data and gravity modeling could be included for a more suitable representation of the collision interface. However, close to the Alpine thrust front general trends are still valuable for kinematic interpretations.

2.5.2. Modeling of the generalized Vienna Basin Transfer Fault

Another large scale tectonic feature is approximated by modeling a generalized Vienna Basin Transfer Fault. It has been proposed by Hinsch et al. (2005) that the recent active transfer fault is rather a linear feature than having a pull-apart step-over geometry like in Miocene times (see also discussion in section 3). In order to represent the principal displacement zone of the Vienna Basin Transfer Fault a single plane has been constructed, even though the real fault system is branching upwards into several splay faults. The generalized fault plane was modeled in GOCAD and constrained by mapped fault cuts in the subsurface, surface fault traces and the seismicity pattern (Fig. 9b), as listed below:

a) Within the Vienna Basin, the position the transfer fault is well determined by the fault cuts in the base of the Miocene surface (Table 1, Fig. 9b) and by the principal displacement zone mapped in seismic data in the southern Vienna Basin (Figs. 4, 9b).

b) South of the Vienna Basin, the surface expression of the fault corresponds to faults mapped in the Mürz Valley. Within the Vienna Basin the seismically principal displacement zone mapped in the subsurface corresponds to morphological fault scarps (scarps a and c, Fig. 7). North of the Vienna Basin, the surface expression of the fault zone is more subtle and difficult to interpret in the digital elevation model. Changes in surface gradients and valley shapes have been utilized to map the position of suspected fault traces.

c) The regional seismicity pattern lines up events along the Mur-Mürz fault, along the eastern border of the Vienna Basin and its linear prolongation towards the Little Carpathians (earthquake data from ZAMG, 2001, 2004). The hypocenters of earthquakes recorded in the last 50 years were utilized and used as constraints to determine the position of the Vienna Basin Transfer Fault.

In a subsequent step the generalized fault plane was vertically delimited by the generalized top of the European Plate, assuming, that the Vienna Basin Transfer Fault is thin-skinned in character and limited to the Alpine thrust wedge (Royden et al., 1983, see also discussion in section 3).
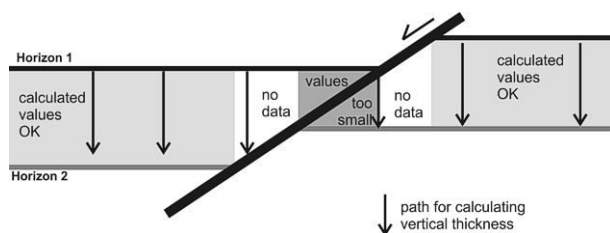

FIGURE 6: Diagram illustrating the calculation of vertical thickness between two horizons. The distance from horizon 1 to horizon 2 is measured and projected onto the lower horizon. With normal offset along a fault, areas without overlap of the two horizons exist. Furthermore areas where the distance is measured across the fault produce too small distances. These values have to be deleted. No data areas on the lower horizon can then be interpolated.

3. Constraints on Miocene to active tectonics

The interpretation of the data presented in this study partly constrains the fault history in Miocene times. The tectonic activity in the central Vienna Basin for the interval Lower Sarmatian to Lower Pannonian is imaged by the syntectonic sedimentation, as mapped by the vertical thickness map (Fig. 5d). Obviously, the Bisamber-Steinberg fault system is the main active fault within this period. This observation is in good agreement with observations from backstripping histories on several wells in the Vienna Basin and deduced fault activity (Wagreich und Schmid, 2002).

Additionally, the interpretation and the faults modeled in this study support a thin-skinned evolution of the Vienna Basin in Miocene times. The apparent increasing age of the fault activity in the Bisamberg and Aderklaa-Bockfliess Fault system, as imaged in Figure 3, can be interpreted as a geometrical indication for thin-skinned normal faulting: The Miocene strata affected by these faults display a drag on the Bisamberg Fault and a rollover syncline in the area of the Aderklaa-Bockfliess Fault System forming an antithetic set of faults, which are regarded as hanging wall collapse structures. The antithetic faults become progressively older towards southeast as shown by the position of the upper fault tips in the sedimentary sequence (Fig. 3). Such behavior is typical for the hanging wall moving over a bend of the underlying listric master fault and through an active axial surface attached to the bend (Xiao and Suppe, 1992). Movement results in a series of antithetic faults with older inactive faults located further off from the master fault, and the youngest (or active) fault attached to the kink of the master fault. The observed rollover syncline and the fault age relationship therefore is regarded to point towards a kink or bend in the fault geometry of the Bisamberg master fault. This kink or bend is likely caused by the conjunction of the main synthetic normal fault and the main detachment system, as inferred from the seismic interpretation (Fig. 3). The geometry of the fault system supports the idea that the normal faults root in the former Alpine floor thrust as a common detachment horizon.

An interesting feature seen in the combined spatial data covering the entire basin is the obvious spatial relationship between the shape of the generalized top of the European Plate and the position of the Vienna Basin. The south-western part of the Vienna Basin Transfer System is the Mur-Mürz Fault (Figs. 1, 10), a major strike-slip fault formed during lateral extrusion of East Alpine crustal blocks (Ratschbacher et al., 1991; Linzer et al, 1997; 2002; Peresson and Decker, 1997). This fault passes over a region, where the top of the European Plate forms a relative high before entering the Vienna Basin ("South Bohemian Basement Spur", Wessely, 1987). The basin itself is situated at a position, where the basement forms a low and retreats towards the north (Fig. 10, note the colour-coding for surface azimuth). At this point, the Leopoldsdorf Fault System represents the main step-over of the pull-apart basin and opens the basin over the retreating basement. Within the basin and at its western border all main faults, the Bisamberg, the Bockfliess and the Steinberg Fault run parallel to the contours of the detachment plane (Fig. 10). These spatial relationships strongly

support the idea that the major faults of the Vienna Basin are guided by and root in the detachment system of the European-Alpine interface, as proposed by Royden et al. (1983). By this
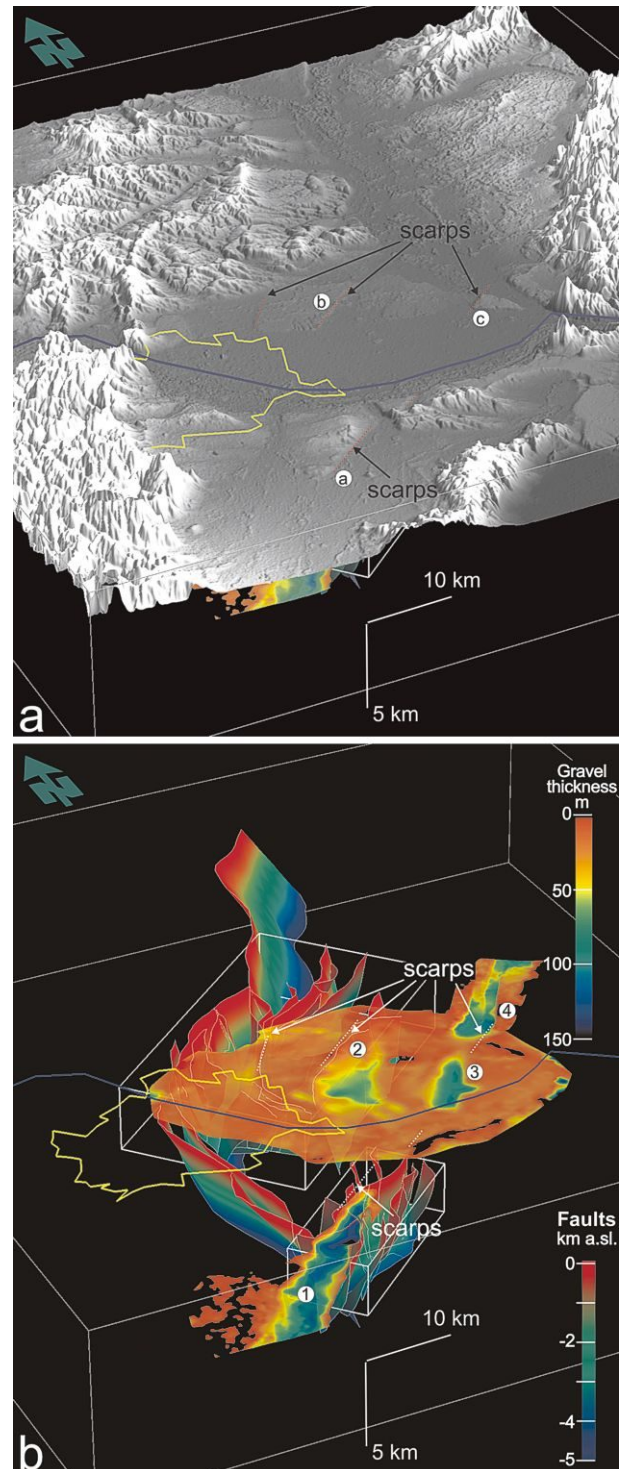

FIGURE 7: a) Oblique view of shaded Digital Elevation Model derived from SRTM data. Elevated areas and terraces in the Vienna Basin are delimited by linear scarps a: Rauchenwarth plateau, b: Gänserndorf terrace, c: Schlosshof terrace (cf. Decker et al., 2005; Hinsch et al., 2005). b) Oblique view of base of Quaternary gravels, colored for gravel thickness and faults interpreted from seismic data. Scarps from Figure 7a are indicated. 1: Mitterndorf Basin, 2: Obersiebenbrunn Basin, 3: Lassee Basin, 4: Zohor Basin.

geometry the pull-apart basin is comparable to the thin-skinned asymmetric basins modeled with analogue materials above a detachment horizon by Rahe et al. (1998). In all their models a long-lived cross-basin fault evolves after the initial basin phase. The fault has changing dip direction and links the strike-slip faults at the entry points of the basin. As shown in Figure 5, the Bockfliess Faults and the Steinberg Fault are the major active faults in the central Vienna Basin in Lower Sarmatian to Lower Pannonian times. These faults can be compared to the major cross-cutting fault system of the mature pull-apart basin of the analogue model. Additionally, this observation suggests a major upper Miocene strike-slip fault leaving the Vienna Basin at its north-eastern tip, which continues into the outer West Carpathians (cf. Decker et al., 1997).

Recent active tectonics of the Vienna Basin seems to differ from the Miocene times in several aspects. Although geological data indicate that most of the major Miocene faults in the Vienna

basin are presently active, the main seismotectonic activity obviously shifted to the eastern border of the basin. This is shown by the distribution of Quaternary fault-bounded basins, geo-morphological features and the seismicity pattern (Figs. 7, cf. Decker et al., 2005 their Fig. 1 for seismicity pattern). Figure 7a displays an oblique view of the SRTM digital elevation model showing the central Vienna Basin as relatively flat area between the Little Carpathian Mountains and the easternmost Alps. The topography inside the basin is dissected by linear scarps (Fig. 7a). Stripping away the DEM allows viewing the distribution of Quaternary gravels underneath (Fig. 7b). The base of Quaternary gravels is color-coded for sediment thickness and slightly translucent to visualize the faults underneath. The fault
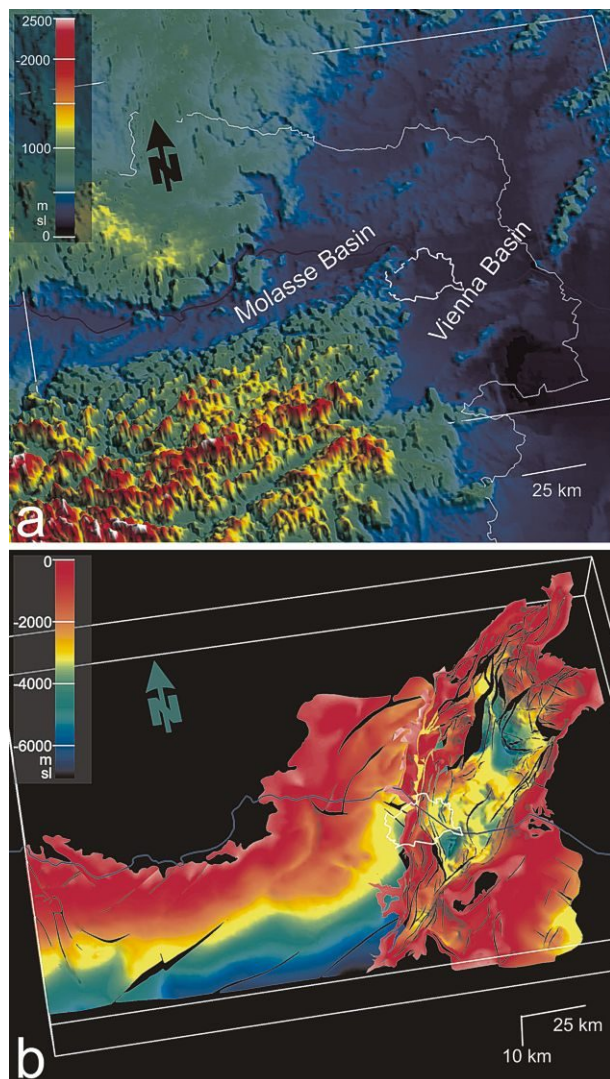

FIGURE 8: a) Oblique view of colored Digital Elevation Model showing the easternmost Eastern Alps, the eastern Molasse Basin and the Vienna Basin. b) Surfaces modeled from published data in the subsurface of the area displayed in e: The base of the Neogene sediments in the Vienna Basin (Kröll and Wessely, 1993) and the base of the Neogene sediments in the Molasse Basin of Lower Austria (Kröll et al., 2001).
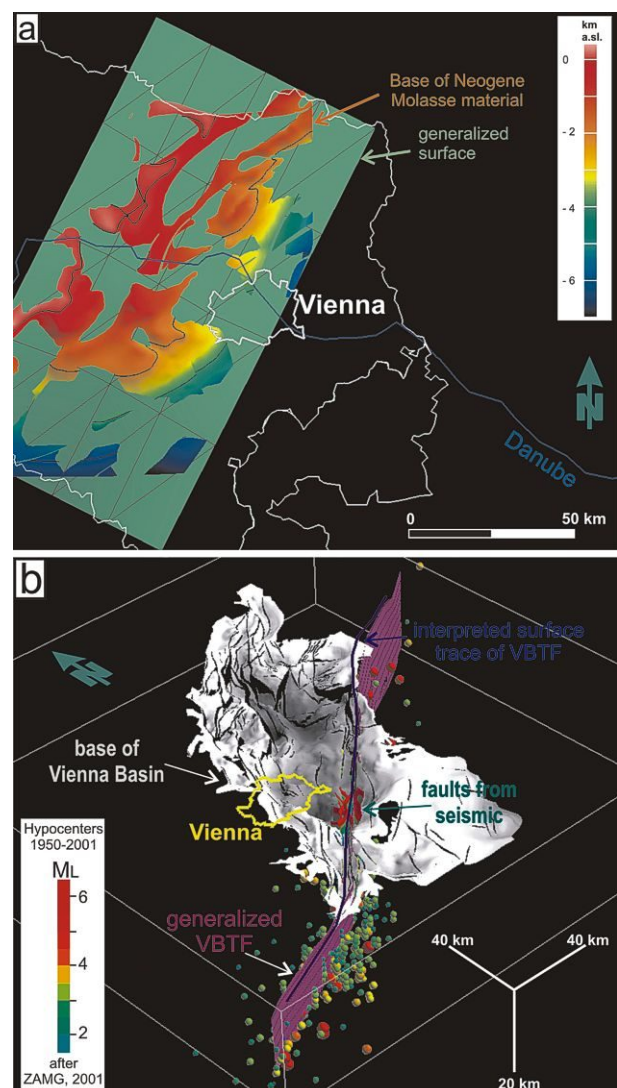

FIGURE 9: a) Construction of surface expressing the general trend of the base of the molasse basin. This surface is considered to approximate the generalized top of the European plate and the trend of the main alpine thrust detachment.
b) Construction of an interpreted generalized Vienna Basin Transfer Fault (VBTF). The fault is constrained by the fault pattern in the base of the Miocene basin fill (grey surface, cf. Fig. 8), by faults picked in reflection seismic data, by the interpreted surface trace from geomorphology (blue) and by hypocenter localizations (colored spheres, adapted after ZAMG, 2001, 2004).

scarps and dissected fluvial terraces clearly demonstrate the Quaternary activity of the underlying faults. The thickest Quaternary gravels accumulated in elongated basins along the eastern boundary of the basin (Fig. 7b, location points 1, 3, 4). These elongated basins are subsided below the drainage level and thus are not of erosional origin. As imaged in the seismic data (Fig. 2a) and visualized in 3-D (Fig. 7b) these basins lie on top of the negative flower structures mapped in the 3-D seismic data and represent the principal displacement zone of the recent Vienna Basin Transfer Fault. Thus, the recent transfer system is a rather straight strike-slip fault at the eastern border of the Vienna Basin than a left stepping pull-apart fault. Such a straight active transfer fault is also indicated by the seismicity pattern, which highlights a linear zone extending from the Vienna Basin into the Little Carpathian Mountains. The generalized Vienna

FIGURE 10: Oblique integrated visualization of all modeled faults (LF = Leopoldsdorf Fault and SF = Steinberg Fault) with generalized VBTF and the surface representing the top of the European platform/Alpine detachment, which is colored for its azimuth. The opening of the Miocene Vienna Basin pull-apart coincides with a change of trend in the European platform surface.

Basin Transfer Fault in Figures 9b and 10 accounts for this interpretation. However, detailed studies on Quaternary and active tectonics of the fault continuing into the Slovak Republic are needed to confirm the proposed model.

The negative flower structures along the fault zone (Fig. 2) are associated with a gentle releasing bend along the main displacement zone. The fault surfaces created for the Moosbrunn area depict the geometry of a negative flower structure with only few fault branches at depth but several intersecting faults in the upper part of the basin. Patterns are typical for a strike-slip system with branch fault geometries indicative for sinistral slip. The branch line at which the basin boundary faults converge into a principal displacement zone (PDZ) lies in a depth of c. 4 km, i.e., close to the base of the Miocene sediments. Such upward branching of basement strike-slip faults entering into sedimentary layers is a common observation at interfaces of heterogeneous materials and has been shown by analogue modeling (Richard et al., 1995). A releasing bend geometry might also explain the continued activity of the normal faults of the Leopoldsdorf system west of the main fault, which results in the tilting of Quaternary fluvial terraces throughout the Vienna Basin (Decker et al., 2005). The normal faults still seem to be kinematically coupled by the existing detachment horizon. Thus, the faults inside the basin can be regarded as an asymmetric part of a crustal scale negative flower structure as the detachment horizon is linked with the transfer fault zone (cf. Hinsch et al., 2005). The pre-existing Miocene faults in the Vienna Basin allow an asymmetric hanging wall collapse towards the releasing bends along the transfer fault.
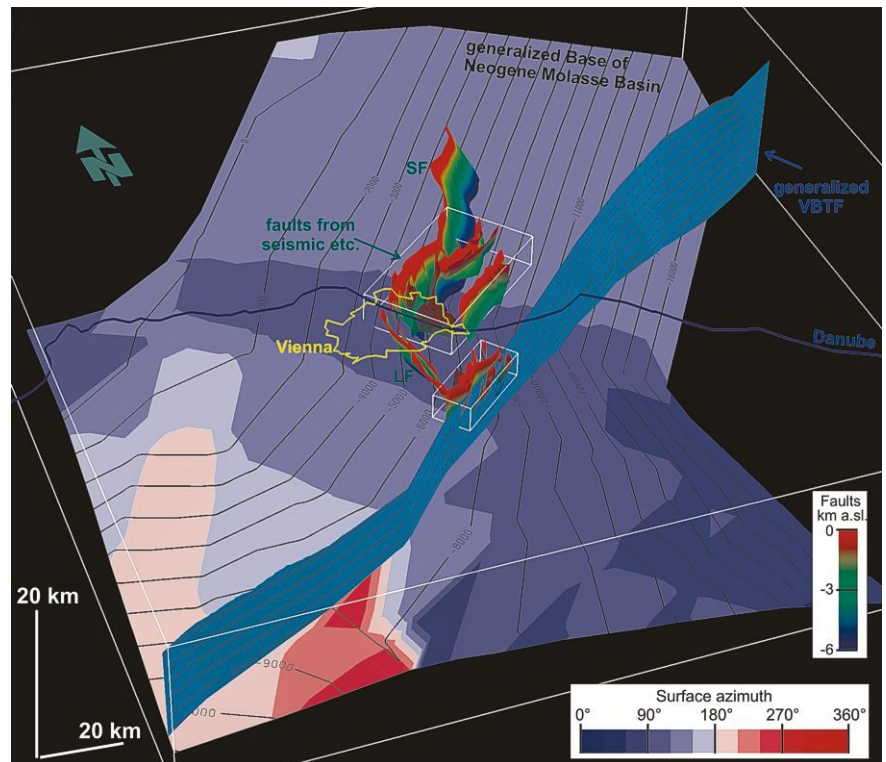
Releasing bend kinematics might well explain the presence of extensional features, even though that the present Pannonian system seems to be mostly under compression (Horvath and Cloetingh, 1996; Bada et al. 2001). Sinistral strike-slip kinematics is in good agreement with the regional NW-SE maximum horizontal stress (Reinecker and Lenhardt, 1999). However, in detail Reinecker and Lenhardt postulate a radial stress pattern around the Bohemian Basement spur, deducted from several stress indicators. Of these, two indicate E-W oriented maximum horizontal stress in and east of the Vienna Basin. This direction would not favor sinsitral strike-slip faulting along the SE-NW trending Vienna Basin Transfer Fault. However, these indicators are of low quality (as stated in Reinecker and Lenhardt, 1999) and contradicting measurements exist, supporting NNW-SSE directions of maximum horizontal stress (Marsch et al., 1990, c.f. Decker et al. 2005). More reliable stress indicators are needed to clarify this contradiction.

Kinematic observations from GPS do indeed support the present activity as sinistral strike slip motion (Grenerczy et al. 2000; Grenerczy, 2002). The crustal block south of the Vienna Basin Transfer Fault (Alpine-North Pannonian or Styrian Block) still or again seems to move in NE directions in respect to the Bohemian Massif. A detailed strain analysis reveals a smoothed SW-NE slip vector (Grenerczy, 2002, his Fig. 15), which is absolutely parallel to the mapped Vienna Basin Transfer Fault. Disregarding possible inaccuracies from the GPS data, the SW-NE vector does not indicate a step-over geometry of the fault system (in which case the vector should be SSW-NNE), thus supporting a model of a straight transfer fault system as presented in this paper.

Acknowledgements

References

Bada, G., Horvath, F., Cloetingh, S., Coblentz, D.D. and Toth, T., 2001. Role of topography-induced gravitational stresses in basin inversion: The case study of the Pannonian basin. Tectonics, 20(3), 343-363.

Berger, E., 1987. Analyse der Funktionsfaktoren des Grund-wasserspeichers Mitterndorfer Senke. Unpublished Report to the Government of Lower Austria, 47 pp.

Decker, K., 1996. Miocene tectonics at the Alpine-Carpathian junction and the evolution of the Vienna Basin. Mitt. Ges. Geol. Bergbaustud., 41, 33-44.

Decker, K., Peresson, H. and Hinsch, R., 2005. Active tectonics and Quaternary basin formation along the Vienna Basin Transfer fault. Quaternary Science Reviews, 24, 305-320.

Decker, K., Nescieruk, P., Reiter, F., Rubinkiewicz, J., Rylko, W. and Tokarski, A.K., 1997. Heteroaxial shortening, strike-slip faulting and displacement transfer in the Polish Carpathians. Przeglad Geologiczny, 45 (10), 1070-1071.

Decker, K. and Peresson, H., 1996. Tertiary kinematics in the Alpine-Carpathian-Pannonian system: links between thrusting, transform faulting and crustal extension, In: G. Wessely and W. Liebl (Editors), Oil and Gas in Alpidic Thrustbelts and Basins of Central and Eastern Europe, EAGE Spec. Publ., 5, 69-77.

DOKW [Österr. Donaukraftwerke AG] 1984. Marchfeld: Lage des maßgeblichen Grundwasserstauers. Unpublished map 1:50.000, Vienna.

Fink, J., 1955. Das Marchfeld. Verhandlungen Geologische Bundesanstalt, Vienna, Spec. Vol. D, 88-116.

Fodor, L., 1995. From transpression to transtension: Oligocene-Miocene structural evolution of the Vienna Basin and the East Alpine-Western Carpathian junction. Tectonophysics, 242, 151-182.

Fuchs, W. and Grill, R. 1984. Geologische Karte von Wien und Umgebung 1:200.000, Geologische Bundesanstalt, Vienna.

Grenerczy, G., 2002. Tectonic processes in the Eurasian-African plate boundary zone revealed by space geodesy. In: S. Stein and J.T. Freymueller (Editors), Plate Boundary Zones. Geodynamic Series, v. 30. American Geophysical Union, 67-86.

Grenerczy, G., Kenyeres, A. and Fejes, I., 2000. Present crustal movement and strain distribution in Central Europe inferred from GPS measurements. Journal of Geophysical Research, 105 (B9), 21835-21846.

Hinsch, R., 2003. Mapping of the 1UP Horizon, Unpublished Internal Report, OMV, Vienna.

Hinsch, R. and Decker, K., 2003. Do seismic slip deficits indicate underestimated seismic potential along the Vienna Basin Transform Fault System? Terra Nova, 15, 343-349.

Hinsch, R., Decker, K. and Wagreich, M., 2005. 3-D mapping of segmented active faults in the southern Vienna Basin. Quaternary Science Reviews, 24, 321-336.

Horváth, F. and Cloetingh, S., 1996. Stress-induced late-stage subsidence anomalies in the Pannonian basin. Tectonophysics, 266, 287-300.

Kröll, A. and Wessely, G., 1993. Wiener Becken und angrenzende Gebiete – Strukturkarte - Basis der tertiären Beckenfüllung. Geologische Themenkarte der Republik Österreich 1:200.000.

Kröll, A., Wessely, G. and Zych, D., 2001. Molassezone Niederösterreich und angrenzende Gebiete - Strukturkarte der Molassebasis. Geologische Bundesanstalt, Vienna.

Kullmann, E., 2000. Three-dimensional geological map of Quaternary sediments of the Slovak part of Zohor-Marchegg groundwater basin in the Borska Lowland. In: P. Malik: Groundwater in the Solovak part of the Vienna Basin: Zohor Depression and „Bezdene" Spring in Plavencky Stvrtok. Excursion Guide, Bratislava 2002, p. 7.

Lankreijer, A., Kovác, M., Cloetingh, S., Pitonák, P., Hloska, M. and Biermann, C., 1995. Quantitative subsidence analysis and forward modelling of the Vienna and Danube Basins: thin-skinned versus thick skinned extension. Tectonophysics, 252, 433-451.

Linzer, H.-G., Moser, F., Nemes, F., Ratschbacher, L. and Sperner, B., 1997. Build-up and dismembering of a classical fold-thrust belt: from non-cylindrical stacking to lateral extrusion in the eastern Northern Calcareous Alps. Tectonophysics, 272, 97-142.

Linzer, H.G., Decker, K., Peresson, H., Dell'Mour, R. and Frisch, W. 2002. Balancing lateral orogenic float of the Eastern Alps. Tectonophysics, 354, 211-237.

Mallet, J.L., 1992. Discrete smooth interpolation in geometric modeling. Computer Aided Design, 24(4), 178-191.

Marsch, F., Wessely, G. and Sackmaier, W., 1990. Borehole-breakouts as geological indications of crustal tension in the Vienna Basin. In: P. Rossmanith (Editor), Mechanics of Joined and Faulted Rock. A.A. Balkema, Rotterdam, pp. 113-120.

Peresson, H. and Decker, K., 1997. The Tertiary dynamics of the Northern Eastern Alps (Austria): Changing paleostresses in a collisional plate boundary. Tectonophysics, 272, 125-157.

Rahe, B., Ferrill, D.A. and Morris, A.P., 1998. Physical analog modeling of pull-apart basin evolution. Tectonophysics 285, 21–40.

Ratschbacher, L., Merle, O., Davy, P. and Cobbold, P., 1991. Lateral extrusion in the Eastern Alps, part I: boundary conditions and experiments scaled for gravity. Tectonics, 10(2), 245-256.

Reinecker, J. and Lenhardt, W.A. 1999. Present-day stress field and deformation in Eastern Austria. Int. Journ. Earth Sciences 88, 532-530.

Richard, P.D., Nylor, M.A. and Koopman, A., 1995. Experimental models of strike-slip tectonics. Petroleum Geoscience, 1, 71-88.

Rögl, F., 1996. Stratigraphic correlation of the Paratethys Oligo-cene and Miocene. Mitt. Ges. Geol. Bergbaustud., 41, 65-74.

Royden, L.H., 1985. The Vienna Basin: A thin-skinned pull-apart basin. In: K. T. Biddle and N. Christie-Blick (Editors). Strike slip deformation, basin formation and sedimentation. SEPM Spec. Publ., 37, pp. 319-338.

Royden, L.H., Horvath, F. and Rumpler, J., 1983. Evolution of the Pannonian Basin System, 1. Tectonics. Tectonics, 2, 63-90.

Royden, L.H., 1988. Late Cenozoic tectonics of the Pannonian Basin system. In: L.H. Royden and F. Horvath (Editors), The Pannonian Basin: a study in basin evolution. AAPG Memoir 45. American Association of Petroleum Geologists and Hungarian Geological Society, Tulsa, Oklahoma, Budapest, pp. 27-48.

Sauer, R., Seifert, P. and Wessely, G., 1992. Guidbook to ex-cursions in the Vienna Basin and the adjacent Alpine-Carpathian thrust-belt in Austria. Mitt. Geol. Ges., Vienna, 85, 1-264.

Strauss, P., Hinsch, R., Harzhauser, M., Wagreich and M., Hölzel, M. 2004. Neogene Sequence stratigraphy from 3-D seismic and outcrops in the Southern Vienna Basin (Austria), EGU General Assembly, Nice, Geophysical Research Abstracts, Vol. 6, 07421.

Strauss, P., Harzhauser, M., Hinsch, R., Wagreich, M., 2005. Sequence Stratigraphy in a classic pull-apart basin (Neogene, Vienna Basin) – a 3D seismic based integrated approach. Geologica Carpathica, in review.

USGS-NIMA, 2003. Shuttle Radar Topography Mission. Computer files. U.S. Geological Survey and The National Imagery and Mapping Agency.

Wagreich, M. and Schmid, H. P., 2002. Backstripping dip-slip fault histories: apparent slip rates for the Miocene of the Vienna Basin. Terra Nova, 14, 163-168

Wessely, G. 1987. Mesozoic and Tertiary evolution of the Alpine-Carpathian foreland in eastern Austria. Tectonophysics 137, 45-49.

Wessely, G., 1988. Structure and development of the Vienna basin in Austria. In: L.H. Royden and F. Horváth (Editors). American Association of Petroleum Geologists, Memoir, 45, pp. 333-346.

Wessely, G., 1993. Geologischer Tiefbau Wiener Becken - Molasse Niederösterreichs, In: F. Brix and O. Schulz (Editors). Erdöl und Erdgas in Österreich, Naturhistorisches Museum Wien und F. Berger, Horn, Austria, Attachment 8.

Wessely, G., Kröll, A., Jiricek, R. and Nemec, F., 1993. Wiener Becken und angrenzende Gebiete - Geologische Einheiten des präneogenen Beckenuntergrundes. Geologische Themenkarte der Republik Österreich, map 1:200.000, Geologische Bundesanstalt, Vienna.

Xiao, H. and Suppe, J., 1992. Origin of rollover. American Association of Petroleum Geologists Bulletin, 76,509-529.

ZAMG, 2001. Earthquake catalogue of felt earthquakes (Austria). Computer File. Central Institute of Meteorology and Geodynamics (ZAMG), Vienna Austria.

ZAMG, 2004. Catalogue of Earthquakes in the Region of the Eastern Alps-Western Carpathians-Bohemian Massif for the period from 1267 to 2004; Attachment to the project >Seismic Active Discontinuities in the Region „Eastern Alps-Western Carpathians-Bohemian Massif"<, based on Geophysical Data and Digital Seismic Records of the Seismic Network "ACORN", W. Lenhardt (Editor) Central Institute for Meteorology and Geodynamics, Department of Geophysics Vienna, Austria and Masaryk University Brno, Faculty of Science Institute of Physics of the Earth Brno, Czech Republic.

R. HINSCH[1),*)], K. DECKER[1)] & H. PERESSON[2)]

[1)] Department of Geological Sciences, University of Vienna, Althanstrasse 14, 1090 Vienna, Austria

[2)] OMV AG Austria, Gerasdorfer Strasse, 1210 Vienna, Austria

[*)] Corresponding author, present address: Rohoel-Aufsuchungs AG (RAG), Schwarzenbergplatz 16, 1015 Vienna, Austria, ralph.hinsch@rohoel.at

Appendix

Map conventions

Modeling and data integration in this project was done using GOCAD (Geological Object Computer Aided Design). GOCAD uses orthogonal X, Y and Z axes to locate atomic objects (i.e. objects defined via discrete vertexes). Therefore, all data in this project is transferred to a metric system with orthogonal projection. We use Transverse Mercator projection (Gauss-Krüger) and the Datum MGI Austria (Militär Geographisches Institut, tie point: Hermannskogel) with a central meridian 16°20´E and false easting of 750.000 but no false northing (Easting thus conforms with the Austrian Bundesmeldenetz [BMN] coordinates); Unlike BMN coordinates we use a 7-digit northing. This is done do avoid confusion of X and Y numbers in sequential coordinate lists in GOCAD.

Depth conversion

Depth conversion of interpretations done on reflection seismic data in two-way-traveltime (TWT) are achieved by the following relation:

$Z = V_0(e^{(kt)} - 1)/k$

with V_0 a starting velocity [m/s]; k a constant, which tunes the increase of velocity with depth, t = OneWayTravel Time [s]. By comparison to time-depth values from wells in the Vienna Basin the parameters V_0 and k have been estimated: V_0 = 1780 and k = 0.7.

This simple approximation provides good results for increasingly compacted sediments down to approximately 3 s TWT. Sharp changes in the velocity structure (e.g. the basement sediment interface) are not represented. Geometries in the basement or deep parts of the basin therefore should be interpreted with care. Original TWT values are saved with the original fault traces and horizon surfaces as point related properties in order to allow future enhancements in depth conversion.

Modeling of GOCAD surfaces

The following paragraph gives a short description on the general procedure for the creation of horizon and fault surfaces in order to provide an idea on the accuracy of the modeled spatial data.

In general, data is imported into GOCAD as X, Y, Z point set. Apart from regular grid data like DEM or horizon data from 3-D seismic interpretation software, data points are heterogeneously distributed (e.g., dense data points along digitized contour lines, heterogeneously distributed well data etc.). In GOCAD, there are two main possibilities of constructing TINs (Triangulated Irregular Networks, called T-surfs in GOCAD). The first approach includes the data points into the surface as vertexes of the triangles (direct triangulation). The second approach utilizes a homogenous triangulated surface, which is smoothly fitted to the data points (interpolation). Direct triangulated surfaces from heterogeneously distributed data often display kinky surfaces with irregular triangles and artifacts. Therefore, the interpolation approach is usually chosen for surface creation.

For interpolated surfaces, there are several factors influencing the geometry of the final surface. The size of the triangles in the initial homogenous triangulated surface is determined by distance of the vertexes of the curve outlining the data and by the densification type used for this initial mesh construction (cf. GOCAD manual). Geometry interpolation of surfaces in GOCAD is based on the DSI algorithm (Discrete Smooth Interpolation; Mallet, 1992), which iteratively aims for a minimization of the curvature in the surface. Interpolation settings influencing the surface shape are the number of iterations for DSI and the fitting factor, which determines whether the final surface is rather smooth or closely fits to the data points (cf. GOCAD manual).

Interpolated surfaces never fit perfectly to the data points. Often the initial surface displays already acquisition inaccuracies and artifacts, which are smoothed out by this procedure. However, sharp changes in the geometry of the real data points might be lost, if not edited manually.

For horizon surfaces it is possible to calculate the vertical error between original data points and interpolated surface. The error value is stored as point-related property with the surface. The allowable error depends on the scale of original data sources (map scale and contour interval, well spacing, seismic resolution and interpretation density) and should be in the order of tens of meters to a hundred meters at maximum. These modeling errors come to several additional sources of inaccuracy like incorrectness of the original data, errors in the digitization and geo-referencing process. Thus, the accuracy of the modeled surfaces is always a function of the original data quality and the purpose for which it was intended.

Presented modeled fault surfaces are somewhat more ambiguous than horizon surfaces.

Faults are mainly interpreted as fault traces on series of sections throughout 3-D seismic data. Individual traces are imported into GOCAD (Fig. 4) and sorted into groups which are interpreted to belong to one fault segment. The grouped fault traces are edited manually where necessary to eliminate doubtful interpretations and to allow for a smooth surface interpolation. Cross-checking with the seismic data at this stage is done where possible and required. Surface construction then utilizes the indirect DSI interpolation approach, smoothing a surface through the grouped fault traces. In the next step, the individual surfaces are extended and intersected. Cutting relationships are defined as interpreted from the seismic data or, where ambiguous, adapted to the overall interpretative conceptual model. In this context, extension of the fault surfaces is also conducted in the Z-direction, where interpretation permits. The upper boundary is defined by the datum of the seismic data (i.e. 130 m a.s.l.) and the lower by the time domain extend of the data (i.e. 3 or 4 sec. TWT, Fig. 4 c, d).

Not all fault traces could be used for the generalized and simplified fault model, thus, at the scale of presentation, not every individual branch fault is represented. Instead some distinctive splays are combined and are now represented by just one fault surface. This results in modeled generalized fault surfaces crossing continuous reflectors in the seismic data at some places. In real world these areas likely represent sediments between en-echelon faults or relay ramps between normal faults (Figs. 3, 4 d).

ZOBODAT - www.zobodat.at

Zeitschrift/Journal: Austrian Journal of Earth Sciences

Jahr/Year: 2004

Band/Volume: 97

Autor(en)/Author(s): Hinsch Ralph, Decker Kurt, Peresson Herwig

Artikel/Article: 3-D seismic interpretation and structural modeling in the Vienna Basin: implications for Miocene to recent kinematics. 38-50